A COMPUTATIONAL STUDY OF HEAT TRANSFER UNDER TWIN TURBULENT SLOT JETS IMPINGING ON PLANAR SMOOTH AND ROUGH SURFACES

by

Peng XU [a,b*]***, Agus P. SASMITO*** [b]***, and Arun S. MUJUMDAR*** [b]

[a] College of Science, China Jiliang University, Hangzhou, China
[b] Department of Mining and Materials Engineering, McGill University, Montreal, Canada

Original scientific paper
DOI: 10.2298/TSCI151130016X

The flow and heat transfer characteristics of twin turbulent slot jets impinging on planar smooth and rough surfaces are examined using a computational fluid dynamics model. The interaction between jets lowers the heat transfer performance of each jet in the zone where the wall jets collide. A single jet performs better than the equivalent twin jet. The average heat transfer under twin jets which are injected alternately so that each one of the pair of jets behaves like a single jet, is found to be better than twin jets issuing simultaneously. It is proposed that alternating jet flows in the twin jet arrangement is a simple novel way to enhance thermal performance of jet pairs. Along with parametric studies of the key flow and geometric parameters, effects of large temperature differences between the jet air and the target surface being heated, and model roughness of the target surface are also evaluated. Interestingly, roughness can lower the heat transfer performance in the impingement zone as the fluid can get trapped in the valleys in the rough surface.

Key words: *gas impingement, twin jets, surface roughness, alternating flows, computational fluid dynamics*

Introduction

Impinging jets of diverse geometric configurations are commonly used in numerous small scale as well as large scale applications, *e. g.*, cooling of electronic components and leading edges of turbine blades, annealing of metal sheets as well as drying of tissue paper, textiles, plywood sheets, extruded foods, coated webs, *etc.* [1-4]. The high heat and mass transfer rates in the impingement zone makes impinging jets very attractive but they also limit some applications requiring uniform heat and mass transfer rates on the target surface. Impinging jets are used in multiplicity so the interactions between jets are very important in determining non-uniformity of the transfer rate distributions.

It has been also shown that the flow and thermal physics of multiple impinging jets on rough surfaces are significantly different from those on smooth target surfaces [5]. However, most majority of mathematical models of multiple impinging jets focus on the heat transfer properties along smooth target surfaces, few research works have been carried out on heat transfer characteristics of impingement on rough surfaces. Several types of rough target surface such as dimpled surface, grooved surface, protrusive surface, rib-roughened target surface, si-

* Corresponding author; e-mail: xupeng@cjlu.edu.cn

nusoidal wave, rectangular wave, triangular wave, *etc.*, have been examined. However, both enhancement and reduction of heat transfer rate on rough surfaces have been reported. Gabour and Lienhard [6] studied an unsubmerged liquid jet on rough surfaces with root-mean-square average roughness heights of 4.7-28.2 μm at Reynolds number of 20,000-84,000, and reported that the local Nusselt number for rough plates can be increased up to 50% compared with that of a smooth wall. Beitelmal and Saad [7] presented that the Nusselt number along the rough surface composed of a circular array of protrusions with 0.5 mm base and 0.5 mm height can be enhanced up to 60% under nozzle-to-plate distance of 1-10 and Reynolds number of 9,600-38,500. The experimental results on air jet impingement onto a circular plate with groves by Sagot *et al.* [8] show that the square cross-section lathe-worked grooves enhance heat transfer rate up to 81% compared with that of smooth plate at Reynolds number of 15,000-30,000. They attributed the heat transfer enhancement to the secondary flows generated insider the grooves. Qiu *et al.* [9] presented a mathematical model on a 2-D confined slot air impinging onto a finned flat plate and reported that the Nusselt number for the finned target surface can be increased up to 50% under Reynolds number of 3,420. Halouane *et al.* [10] conducted a 3-D numerical simulation on the turbulent axisymmetric round jet issuing into a cylindrical hot cavity by Reynolds stress turbulence model, and they found that the average Nusselt number along the cavity walls increases considerably with the jet exit Reynolds number compared with corresponding cases for impinging jet on a flat plate. Xu *et al.* [11] presented an entropy generation analysis on the single impinging jet onto a rough surface, and indicated that the average heat transfer rate can be enhanced by the rough surface.

However, Ekkad and Kontrovitz [12] stated that the in-line and staggered dimple configurations in air impingement produce lower heat transfer coefficients compared with those of a smooth target surface under jet flow Reynolds number of 4,800-14,800, and they ascribed this to the bursting phenomenon of the flow insider the dimples which breaks up the impingement core. However, the bursting phenomenon in channel flows produces local turbulence, flow separation, and reattachment. Lou *et al.* [13] examined the local heat transfer rate of the confined jet impingement onto sine wave, rectangular wave, and triangular wave, respectively. Their numerical results at Reynolds number of 80 show that the model rough target plates can lower the heat transfer from the target plate to the impinging fluid in the laminar regime. They proposed that the presence of recirculation bubbles in the cavities formed by the trapped working fluid can reduce the local heat transfer rate, however, the effect of rough surface on the flow and thermal boundary layers and the extended heat transfer area were not included in their analysis. The numerical study by Zhang *et al.* [14] indicate that the application of dimpled and protrusive surface in synthetic jet impingement has marginal effect on cooling effect for large frequency of synthetic jet (320 Hz).

It can be found that there are a great number of parameters that take important effect on the fluid flow and thermal performance of the jet impingement onto a rough surface. It is still a challenge to explore the heat transfer properties and physical mechanisms of gas jet impingement on a rough surface in a specific circumstance. Therefore, the current work aims to investigate the flow and heat transfer characteristics of gas impingement on planar smooth and rough surfaces. A 2-D twin-jet gas impingement on a sinusoidal wave target surface will be modeled by computational fluid dynamics method. The gas flow characteristics and heat transfer performances of the jet impingement on a rough surface are examined and compared with that of smooth surface. The effect of jet Reynolds number, large temperature difference between jet flow and impinging target, jet impingement dimension, surface roughness as well as intermittent mode of twin jets on the heat transfer rate are also analyzed and presented in detail.

Mathematical modeling

Since in industrial practice, it is essential to use multiplying of jets, it is also necessary to design the exhaust systems carefully to minimize interaction between adjacent jets which affect the thermal performance adversely due to so called *cross-flow* effect. Spent fluid from the upstream jet mixes with the downstream jet prior to impingement and reduce the driving force for heat/mass transfer. In this study, the impingement heat transfer on smooth as well as rough planar surfaces due to twin turbulent slot jets was examined. The flow configuration is shown in fig. 1, a 2-D semi-confined twin-jet gas impingement with slot nozzle width of w on a sinusoidal wave rough surface was studied. In order to simplify computations, two symmetrical jets with separation of S and height of H were modeled. A sinusoidal wave was employed here to simulate the rough impinging target surface, which was composed of a section of wavy surfaces with same wave height (h) and wavelength (s). The amplitude and frequency defined as $a = h/s$ and $f = L/s$ were used to characterize surface roughness, respectively. The impinging surface with length of L contains a rough surface section of L_r and smooth surface with length of L_s. In order to examine the effect of surface roughness on the heat transfer performance, the lengths of rough and smooth surface were set as $L_r/w = 10$ and $L_s/w = 90$. The geometric dimensions and parameters were summarized in tab. 1, and the temperature-dependent air properties [15] were listed in tab. 2.

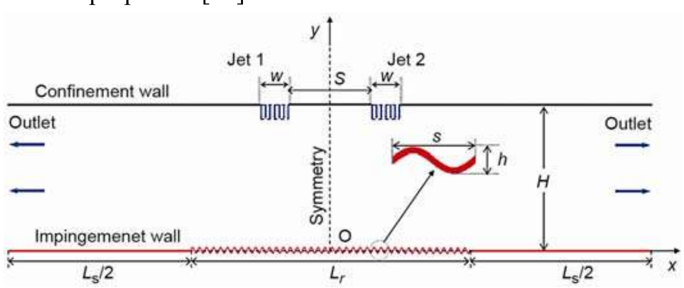

Figure 1. A schematic of the 2-D twin-jet of slot nozzles onto a sinusoidal wave surface

Table 1. Geometric dimensions and parameters of the twin-jet impingement

Parameter	Value	Parameter	Value
Length of system	$L/w = 100$	Roughness frequency	$f = 100\sim400$
Rough surface length	$L_r/w = 10$	Reynolds number	Re = 2,000~14,000
Smooth surface length	$L_s/w = 90$	Atmospheric temperature, [K]	$T_\infty = 300$
Nozzle-to-plate distance	$H/w = 2\sim7$	Temperature of jet flow, [K]	$T_\mathrm{f} = 350\sim400$
Jet nozzle separation	$S/w = 1\sim6$	Temperature of impingement wall, [K]	$T_\mathrm{w} = 300$
Roughness amplitude	$a = 0\sim40\%$	Temperature difference, [K]	$\Delta T = 50\sim100$

The air flow and convective heat transfer in the twin turbulent impinging jets were determined by numerically solving the following equations for conservation of mass, momentum, and energy in the Cartesian co-ordinate system:

$$\frac{\partial u_i}{\partial x_i} = 0 \tag{1}$$

Table 2. Thermophysical properties of air

Property	Relationship
Density, [kgm^{-3}]	$\rho = 3.07534 - 0.00887T + 8.847515 \cdot 10^{-6}T^2$
Dynamic viscosity, [kgm^{-1}s^{-1}]	$\mu = 1.45073 \cdot 10^{-6} + 6.62887 \cdot 10^{-8}T - 3.1933 \cdot 10^{-11}T^2$
Thermal conductivity, [Wm^{-1}K^{-1}]	$\lambda = -2.82567 \cdot 10^{-4} + 9.91365 \cdot 10^{-5}T - 3.57511 \cdot 10^{-8}T^2$
Specific heat, [Jkg^{-1}K^{-1}]	$c_p = 1032.306 - 0.2104T + 4.12739 \cdot 10^{-4}T^2$

$$\rho u_j \frac{\partial u_i}{\partial x_j} = -\frac{\partial P}{\partial x_i} + \frac{\partial}{\partial x_j}\left[\mu\left(\frac{\partial u_i}{\partial x_j} + \frac{\partial u_j}{\partial x_i}\right) - \rho\overline{u_i' u_j'}\right] + \rho g_i \tag{2}$$

$$\rho u_j \frac{\partial (T)}{\partial x_j} = \frac{\partial}{\partial x_j}\left[\frac{\lambda}{c_p}\frac{\partial T}{\partial x_j} - \rho\overline{u_j' T'}\right] \tag{3}$$

The flow and thermal fields were computed by the finite volume computational fluid dynamics code Fluent 16.1. Several turbulence models such as k-ε models, k-ω models, Reynolds stress model, low-Reynolds models, *etc.* have been proposed for highly anisotropic turbulence components in turbulent impinging jet [16-18]. Among these turbulence models, RNG k-ε turbulence model is numerically robust and relatively fast, which has been proven to be effective in modeling this type of complex flow in impinging and opposed jets [17, 18]. It is thus recommended for moderate accuracy in modeling jet impingement heat transfer [1]. As shown in fig. 2(a), the numerical predictions by RNG k-ε turbulence model show acceptable agreement with that of experimental results [19]. Thus, RNG k-ε turbulence model was used to model turbulence in subsequent simulations.

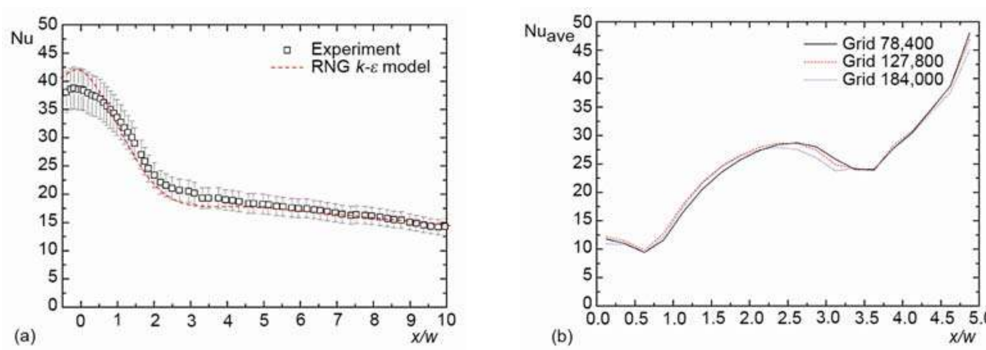

Figure 2. (a) Model validation with experimental data [19] at $H/w = 5$ and Re = 5,500; (b) grid-independence test under $H/w = 5$, $S/w = 3$, $a = 40\%$, $f = 400$, Re = 6,000, and $\Delta T = 100$ K

The boundary conditions in the current model were specified as: uniform velocity, temperature, turbulent kinetic energy and energy dissipation rate profiles were imposed at jet nozzle exits, pressure outlet boundary condition was applied at outlet planes, confinement surface and impingement surface with no-slip condition were considered to be adiabatic ($q = 0$) and isothermal ($T = T_w$), respectively, large temperature differences between the jet flow and drying surface $\Delta T = T_f - T_w$ were used ($\Delta T > 50$ K). The semi-implicit method for pressurelinked equations algorithm and pressure staggering option scheme were employed for the pressure-velocity coupling and pressure interpolation. A second upwind discretization scheme was adopted considering the stability of solution convergence. The convergence criterions for the normalized residuals of energy and other variables were taken as 10^{-7} and 10^{-4}, respectively. A non-uniform structured grid with increased grid density along the impinging target was used. Grid-sensitivity studies have been carried out to obtain the optimum grid resolution which provides a grid-independent solution. Figure 2(b) shows one set of results about the effect of grid density on the averaged Nusselt number under $H/w = 5$, $S/w = 3$, $a = 40\%$, $f = 400$, Re = 6,000, and $\Delta T = 100$ K. It can be clearly seen that a grid density of 78,400 provides satisfactory solution for the example shown.

Results and discussion

The Reynolds number can be defined as $\mathrm{Re} = \rho u_\mathrm{f} w/\mu$ according to the jet flow velocity u_f and slot width w. The local Nusselt number for an isothermal impingement surface was defined:

$$\mathrm{Nu} = \frac{q}{T_\mathrm{f} - T_\mathrm{w}} \frac{w}{\lambda} \tag{4}$$

where $\Delta T = T_\mathrm{f} - T_\mathrm{w}$ is the temperature difference between gas jet flow and impinging surface, and λ is the thermal conductivity of jet fluid. The area-averaged Nusselt number was calculated by:

$$\mathrm{Nu}_\mathrm{ave} = \frac{1}{A} \int \mathrm{Nu} \, \mathrm{d}A \tag{5}$$

Firstly, the convective heat transfer property of the twin impinging jets on a rough surface was compared with that of smooth surface, and single jet cases. Figures 3(a) and (b) show the Nusselt number distribution along the impinging surface for the twin impinging jets on a rough surface, twin impinging jets on a smooth surface and single jet on a rough surface at $H/w = 5$, Re = 6,000, and $\Delta T = 100$ K. As shown in fig. 3(a), the local Nusselt number distribution for the twin impinging jets on a sinusoidal rough surface is a fluctuation curve with clear peaks and valleys. The comparison of area-averaged Nusselt number between the rough

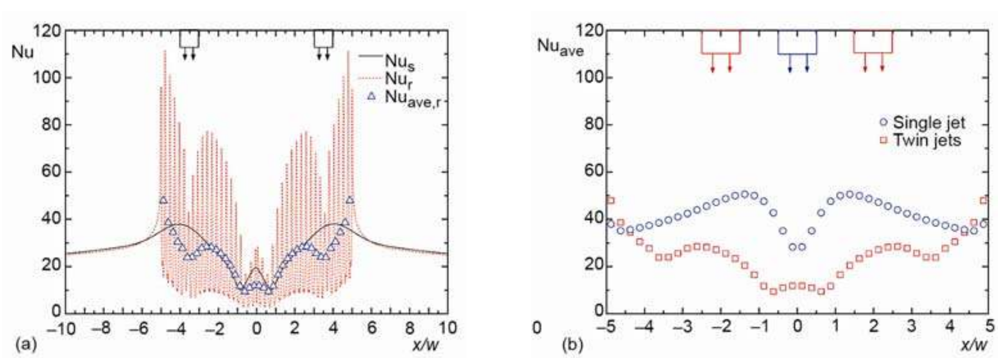

Figure 3. (a) The Nusselt number distributions along the smooth and rough impinging surfaces in the twin impinging jets under *H*/*w* = 5, *S*/*w* = 3, *a* = 40%, *f* = 400, Re = 6,000, Δ*T* = 100 K; (b) averaged Nusselt number on a rough surface (*a* = 40% and *f* = 400) for twin impinging jets (*S*/*w* = 3) and central single jet at *H*/*w* = 5, Re = 6,000, and Δ*T* = 100 K

and smooth impinging target surfaces indicates that the heat transfer rate around the stagnation points below the jet nozzles and secondary stagnation point between adjacent jets can be lowered by the rough surface. For the twin-jet impingement, the wall jets of two adjacent flows may collide, resulting in secondary stagnation region, fig. 4(a). It can be seen in fig. 4(b) that the injected air can be trapped in the cavities between the crests of the wave of the rough target surface, thus, the stagnation effects can be amplified by the sinusoidal rough surfaces. However, the area-averaged Nusselt number in the wall jet region can be slightly increased by the rough surface, which can be ascribed to the extended heat transfer area by the sinusoidal rough surface and thin boundary layer on the wave crest. While, the local heat transfer rate around stagnation point below the jet nozzle is decreased by the rough surface for the single impinging jet, fig. 3(b). It is clear in fig. 3(b) that the heat transfer rate for the twin impinging jets on a rough surface is lower than that of single jet on a rough surface. The fountain-like flow structure in twin impinging jets may cause momentum exchange with the free jet-shearing layer, and the surface heat transfer rate can be thus decreased [1, 20].

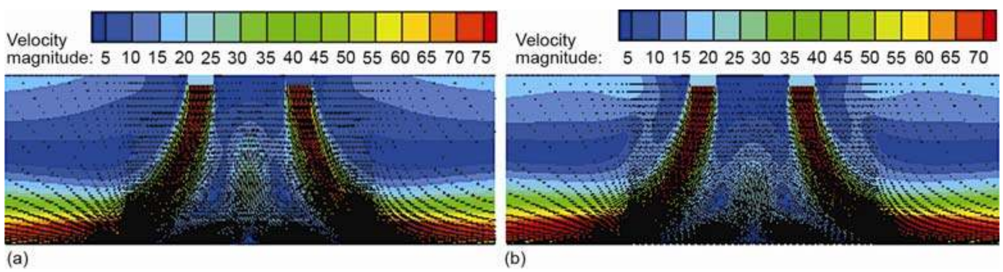

Figure 4. The contours of velocity magnitude with velocity vectors in the twin impinging jets on (a) smooth and (b) rough surfaces at *H*/*w* = 5, *S*/*w* = 3, Re = 6,000, and Δ*T* = 100 K

In the following parameter studies, the effect of jet flow Reynolds number ranging from 2,000 to 14,000, temperature difference between jet flow and impinging surface from 50-100 K, nozzle-to-plate distance from 2-7, jet separation from 1-6, roughness amplitude ranging from 0-40% and roughness frequency from 100-400, on heat transfer rates were examined in detail. A dimensionless enhancement factor ε_{H} was defined as the ratio of the averaged Nusselt number of rough surface to that of smooth surface.

$$\varepsilon_{\mathrm{H}} = \frac{\mathrm{Nu}_{\mathrm{ave,r}}}{\mathrm{Nu}_{\mathrm{ave,s}}} \tag{6}$$

Because of the symmetry of the twin impinging jets, only the numerical results in half of the computational domain were shown in figs. 5-8.

As shown in fig. 5(a), the local Nusselt number for the twin impinging jets on a rough surface can be increased with the increase of Reynolds number of jet flow. Also, the stagnation effect can be clearly strengthened by increasing jet flow Reynolds number. The non-uniformity of local Nusselt number increases as Reynolds number increases. It can be found in fig. 5(b) that the enhancement factor for low Reynolds number (Re = 2000) is below 1.0, which means that the local heat transfer rate for the rough surface is lower than that of smooth surface. At high Reynolds number, the enhancement factors in the wall jet zones are larger than 1.0. However, the enhancement factor around stagnation points is still lower than 1.0 at high Reynolds number as the stagnation effect can be amplified by increased jet flow

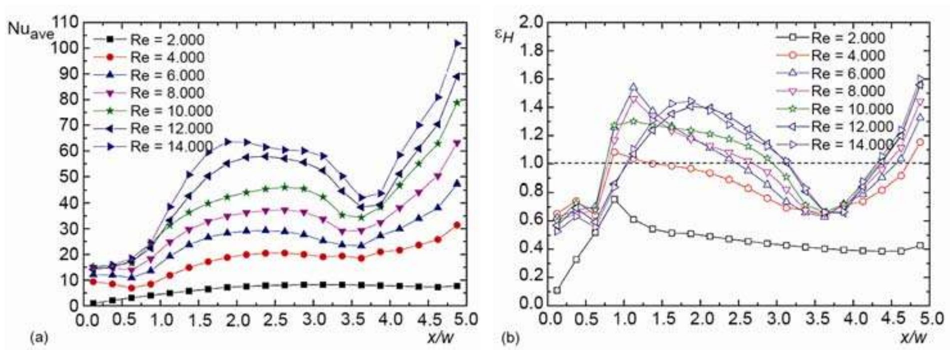

Figure 5. Effect of Reynolds number on the Nusselt number distributions along rough surface (a) and enhancement factor (b) under *H*/*w* = 5, *S*/*w* = 3, *a* = 40%, *f* = 400, and Δ*T* = 100 K

Reynolds number. Figure 6 shows the effect of temperature difference between jet flow and impinging surface on the Nusselt number and enhancement factor at *H*/*w* = 5, *S*/*w* = 3, *a* = 40%, *f* = 400, and Re = 6,000. It can be found that the average Nusselt number can be slightly enhanced by increasing temperature difference. While, the effect of temperature difference on the enhancement factor is marginal.

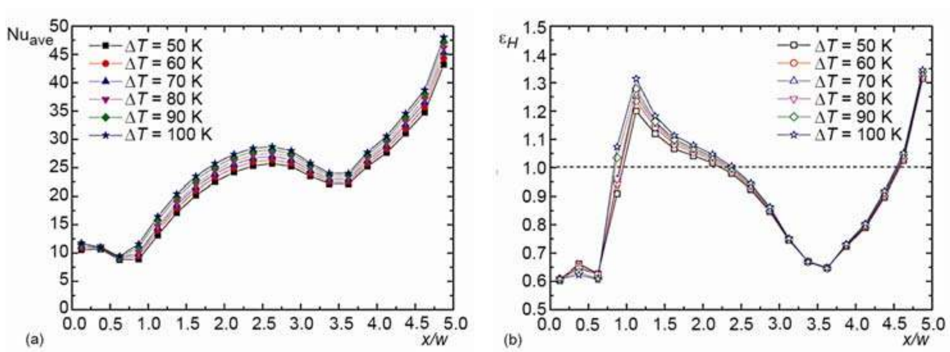

Figure 6. Effect of temperature difference between jet flow and impinging surface on the Nusselt number distributions along the rough impinging surface (a) and enhancement factor (b) under *H*/*w* = 5, *S*/*w* = 3, *a* = 40%, *f* = 400, and Re = 6,000

The geometric dimension and assemble of jet nozzles indicate significant effect on the impinging flow and heat transfer rate. It can be seen in fig. 7(a) that the local Nusselt number along the rough surface decreases with the increase of nozzle-to-plate distance. Also, the stagnation point shifts outwards from the center line of adjacent jets with increased nozzle-to-plate distance. This can be explained as that the injected air flows tend to move outwards during the impingement with increased nozzle-to-plate distance because of the interaction of adjacent jet flows and high pressure between the adjacent jets. As the locations of jet nozzles change along horizontal direction with the increase of jet separation, the stagnation point moves along horizontal direction, fig. 7(b). The jet separation takes significant effect on the local heat transfer rate of the twin impinging jets on a rough surface, especially for the area between adjacent jets. The local Nusselt number between the adjacent jets can be decreased with the increase of jet separation.

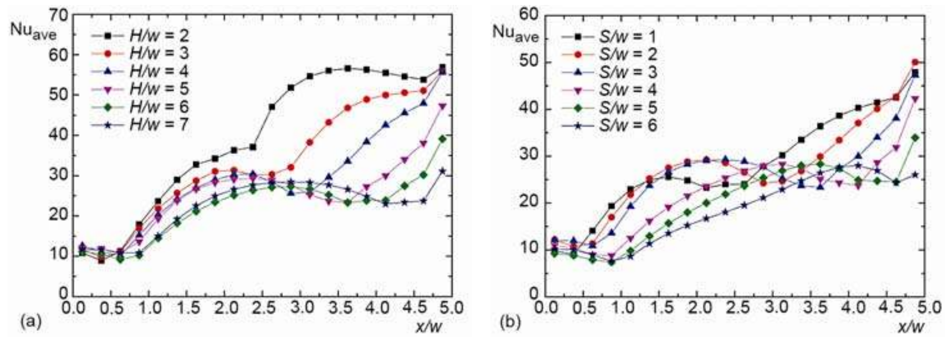

Figure 7. Effect of geometric dimensions on the averaged Nusselt number along the rough surface (a = 40% and f = 400) under Re = 6,000 and ΔT = 100 K; (a) nozzle-to-plate distance with S/w = 3, (b) jet separation with H/w = 5

The effect of surface roughness on the Nusselt number were examined and shown in fig. 8. It can be clearly seen in figs. 8(a) and (b) that the averaged Nusselt number along the rough surface around the stagnation points are lower than that of smooth surface. The Nusselt number along the rough surface around the stagnation points can be further reduced with increased surface roughness amplitude and frequency. A larger value of the amplitude (larger wave height) and frequency (smaller wavelength) means rougher target surface as the ratio asperity height to spacing (h/s) is larger. Thus, the effect of the trapped air and increment of boundary layer thickness in the cavities between the wave crests of the rough surface can be increased as the surface roughness increases. In the wall jet zone, the Nusselt number can be gradually enhanced with increased surface roughness amplitude and frequency. It can be ascribed to the effect of extended heat transfer area by the rough surface and thinner boundary layer on the wave crests.

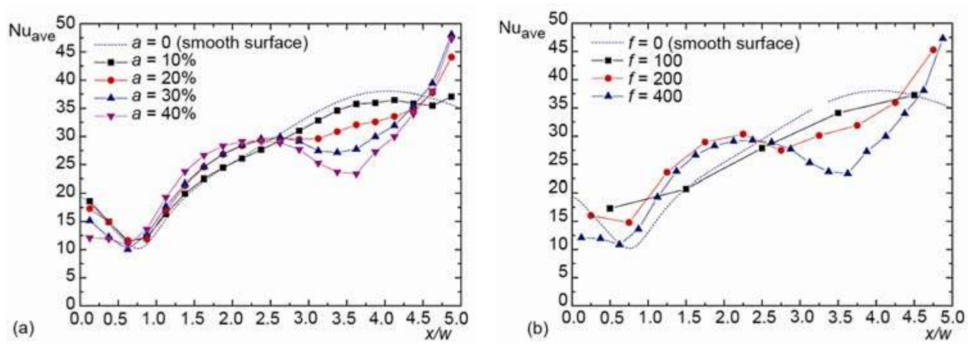

Figure 8. Surface roughness effect on the area-averaged Nusselt number at H/w = 5, S/w = 3, Re = 6,000, ΔT = 100 K; (a) amplitude of rough surface with fixed frequency (f = 400), (b) frequency with fixed amplitude (a = 40%)

It is believed that the intermittent impinging jet may induce higher turbulence, larger vortices, increased flow entrainment and mixing promoted by flow instabilities as well as reduced instantaneous hydrodynamic and thermal boundary layers in the flow domain [21-23]. Thus, the intermittent twin jets which are injected alternately onto a rough surface were also proposed to improve the heat transfer performance. Figure 9 shows the averaged Nusselt number for the simultaneous and alternating twin-jet impingement on planar smooth and rough surfaces under Re = 6,000 and ΔT = 100 K. For both cases of smooth and rough surfaces, the alternating jet flows can improve the heat transfer performance compared with simultaneous cases. The application of alternating jet flows in the twin impinging jets onto a rough surface can effectively eliminate the secondary stagnation point between adjacent jets. The intermittent (alternating) twin impinging jets on a rough surface shows evident advantages in both of heat transfer rate and temperature uniformity. It can be also found in fig. 9 that the influence of rough surface on heat transfer performance of simultaneous impinging jets is slight, while the alternating impinging jets on a rough surface behave completely different from that on a smooth surface. That is the surface roughness has very different effects on simultaneous and alternating impingement flow and heat transfer. It is noted that this numerical results are consistent with the experimental findings by Herwig and Middelberg [24]. And also, adjusting the dimensions of jet nozzles (asymmetric and non-uniform jet array) can be a potential way to improve the uniformity of impingement surface heat transfer rate and temperature [25].

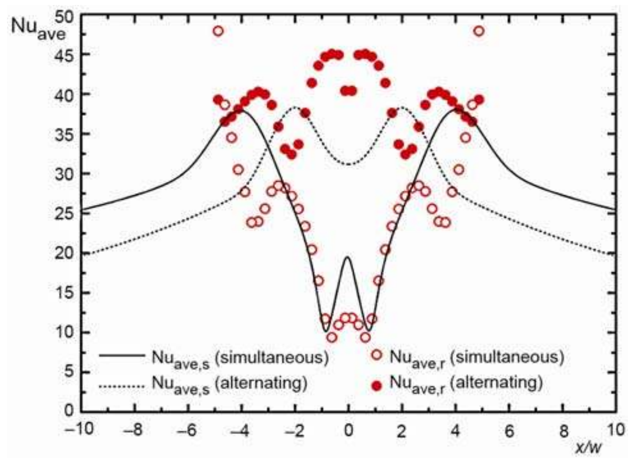

Figure 9. The averaged Nusselt number of the twin impinging jets (H/w = 5 and S/w = 3) on a smooth surface and rough surface (a = 40%, f = 400) under Re = 6,000 and ΔT = 100 K

Conclusions

The twin gas impinging jets on planar smooth and rough target surfaces have been numerically studied in the current work. The fluid flow and heat transfer in the twin slot jets on a rough surface have been compared with that of smooth surface and single impinging jet. The results show that the heat transfer performance for the twin impinging jets on a rough surface is significantly different from that of smooth surface. The surface heat transfer rate can be decreased in the twin impinging jets by the fountain-like flow structure between two adjacent impinging flows. The rough surface can amplify the stagnation effect of the twin impinging jets, which can be increased by increased jet flow Reynolds number and surface roughness. The Nusselt number around stagnation points can be lowered as the roughness amplitude and frequency increase, while the Nusselt number in the wall jet zone can be enhanced with the increase of surface roughness. It has been shown that alternating jet flows in the twin jet arrangement can evidently improve the heat transfer performance, which may have great application potential in cooling of electronic components and drying of sheet products, *etc.*

Acknowledgments

This work was jointly supported by National Natural Science Foundation of China through Grant nos. 11202201, Zhejiang Provincial Natural Science Foundation of China through Grant numbers LY16A020002 and LQ16E060002, and China Scholarship Council.

Nomenclature

A – area, [m^2]
a – roughness amplitude (= h/s)
c_p – specific heat, [Jkg^{-1}K^{-1}]
f – roughness frequency (= L/s)
g – gravity acceleration, [ms^{-2}]
h – asperity height, [m]
H – nozzle-to-plate distance, [m]
L – impinging surface length, [m]
Nu – Nusselt number, eq. (4)
P – static pressure, [Pa]
q – heat flux density, [Wm^{-2}]
Re – Reynolds number (= $\rho uw/\mu$)
S – jet separation, [m]
s – asperity spacing, [m]
T – temperature, [K]
ΔT – temperature difference, [K]
u – velocity, [ms^{-1}]
w – slot width, [m]
x, y – Cartesian co-ordinates, [m]

Greek symbols

ε_H – heat transfer enhancement factor, [–]
λ – thermal conductivity, [Wm^{-1}K^{-1}]
μ – dynamic viscosity, [kgm^{-1}s^{-1}]
ρ – density, [kgm^{-3}]

Superscripts

$'$ – fluctuation

Subscripts

ave – area-averaged
f – gas jet flow
i, j – indices in Einstein summation convention
r – rough target surface
s – smooth target surface
w – impingement wall
∞ – atmospheric

References

[1] Zuckerman, N., Lior, N., Jet Impingement Heat Transfer: Physics, Correlations, and Numerical Modeling, *Advances in Heat Transfer, 39* (2006), pp. 565-631
[2] Mujumdar, A. S., *Impingement Drying, Handbook of Industrial Drying* (Ed. A. S. Mujumdar), CRC Press, New York, USA, 2014, pp. 371-380
[3] Specht, E., Impinging Jet Drying, *Modern Drying Technology Vol. 5: Process Intensification* (Eds. E. Tsotsas and A.S. Mujumdar), Wiley-VCH, Weinheim, Germany, 2014, pp. 1-24
[4] Xiao, H.-W., Mujumdar A. S., Impingement Drying: Applications and Future Trends, *Drying Technologies for Foods: Fundamentals & Applications* (Eds. P. K. Nema, *et al.*), New India Publishing Agency, New Delhi, India, 2015, pp. 279-299
[5] Behnia, M., *et al.*, Accurate Modeling of Impinging Jet Heat Transfer, Annual Research Briefs, Center for Turbulence Research, Stanford University, Stanford, Penn., USA, 1997, pp. 149-164
[6] Gabour, L. A., Lienhard, J. H., Wall Roughness Effects on Stagnation-Point Heat Transfer Beneath an Impinging Liquid Jet, *Journal of Heat Transfer*, *116* (1994), 1, pp. 81-87
[7] Beitelmal, A. H., Saad, M. A., Effects of Surface Roughness on the Average Heat Transfer of an Impinging Air Jet, *International Communications in Heat and Mass Transfer, 27* (2000), 1, pp. 1-12
[8] Sagot, B., *et al.*, Enhancement of Jet-to-Wall Heat Transfer Using Axisymmetric Grooved Impinging Plates, *International Journal of Thermal Sciences, 49* (2010), 6, pp. 1026-1030
[9] Qiu, S., *et al.*, Enhanced Heat Transfer Characteristics of Conjugated Air Jet Impingement on a Finned Heat Sink, *Thermal Science*, 2015, DOI: 10.2298/TSCI141229030Q
[10] Halouane, Y., *et al.*, Turbulent Heat Transfer for Impinging Jet Flowing Insider a Cylindrical Hot Cavity, *Thermal Science*, *19* (2015), 1, pp. 141-154
[11] Xu, P., *et al.*, Heat Transfer and Entropy Generation in Air Jet Impingement on a Model Rough Surface, *International Communications in Heat and Mass Transfer, 72* (2016), March, pp. 48-56
[12] Ekkad, S. V., Kontrovitz, D., Jet Impingement Heat Transfer on Dimpled Target Surfaces, *International Journal of Heat and Fluid Flow*, *23* (2002), 1, pp. 22-28
[13] Lou, Z. Q., *et al.*, Effects of Geometric Parameters on Confined Impinging Jet Heat Transfer, *Applied Thermal Engineering*, *25* (2005), 17-18, pp. 2687-2697
[14] Zhang, D., *et al.*, Numerical Investigation of Heat Transfer Performance of Synthetic Jet Impingement onto Dimpled/Protrusioned Surface, *Thermal Science*, *19* (2015), Suppl. 1, pp. S221-S229
[15] Welty, J., *et al.*, *Fundamentals of Momentum, Heat, and Mass Transfer* (5th ed), John Wiley & Sons, New York, USA, 2008, pp. 678-690

[16] Hofmann, H. M., *et al.*, Calculations of Steady and Pulsating Impinging Jets-An Assessment of 13 Widely used Turbulence Models, *Numerical Heat Transfer, Part B: Fundamentals, 51* (2007), 6, pp. 565-583
[17] Sharif, M. A. R., Mothe, K. K., Parametric Study of Turbulent Slot-Jet Impingement Heat Transfer From Concave Cylindrical Surfaces, *International Journal of Thermal Science*, *49* (2010), 2, pp. 428-442
[18] Parham, K., *et al.*, A Numerical Study of Turbulent Opposed Impinging Jets Issuing from Triangular Nozzles with Different Geometries, *Heat and Mass Transfer, 47* (2011), 4, pp. 427-437
[19] Mladin, E. C., Zumbrunnen, D. A., Local Convective Heat Transfer to Submerged Pulsating Jets, *International Journal of Heat and Mass Transfer, 40* (1997), 14, pp. 3305-3321
[20] Taghinia J., *et al.*, Numerical Investigation of Twin-Jet Impingement with Hybrid-Type Turbulence Modeling, *Applied Thermal Engineering, 73* (2014), 1, pp. 650-659
[21] Xu, P., *et al.*, Turbulent Impinging Jet Heat Transfer Enhancement due to Intermittent Pulsation, *International Journal of Thermal Science, 49* (2010), 7, pp. 1247-1252
[22] Xu, P., *et al.*, A Study on the Heat and Mass Transfer Properties of Multiple Pulsating Impinging Jets, *International Communications in Heat and Mass Transfer, 39* (2012), 3, pp. 378-382
[23] Gitan, A. A., *et al.*, Development of Pulsating Twin Jets Mechanism for Mixing Flow Heat Transfer Analysis, *The Scientific World Journal, 2014* (2014), ID pp. 767614
[24] Herwig, H., Middelberg, G., The Physics of Unsteady Jet Impingement and Its Heat Transfer Performance, *Acta Mechanica*, *201* (2008), 1, pp. 171-184
[25] Shariatmadar, H., *et al.*, Experimental and Numerical Study on Heat Transfer Characteristics of Various Geometrical Arrangement of Impinging Jet Arrays, *International Journal of Thermal Science, 102* (2016), Apr., pp. 26-38

Paper submitted: November 3, 2015
Paper revised: December 2, 2015
Paper accepted: January 11, 2016